



This is a repository copy of *The early dynamical evolution of cool, clumpy star clusters*.

White Rose Research Online URL for this paper:
<http://eprints.whiterose.ac.uk/120257/>

Version: Accepted Version

Article:

Allison, R.J., Goodwin, S.P., Parker, R.J. et al. (2 more authors) (2010) The early dynamical evolution of cool, clumpy star clusters. *Monthly Notices of the Royal Astronomical Society*, 407 (2). pp. 1098-1107. ISSN 0035-8711

<https://doi.org/10.1111/j.1365-2966.2010.16939.x>

Reuse

Unless indicated otherwise, fulltext items are protected by copyright with all rights reserved. The copyright exception in section 29 of the Copyright, Designs and Patents Act 1988 allows the making of a single copy solely for the purpose of non-commercial research or private study within the limits of fair dealing. The publisher or other rights-holder may allow further reproduction and re-use of this version - refer to the White Rose Research Online record for this item. Where records identify the publisher as the copyright holder, users can verify any specific terms of use on the publisher's website.

Takedown

If you consider content in White Rose Research Online to be in breach of UK law, please notify us by emailing eprints@whiterose.ac.uk including the URL of the record and the reason for the withdrawal request.



eprints@whiterose.ac.uk
<https://eprints.whiterose.ac.uk/>

The early dynamical evolution of cool, clumpy star clusters

Richard J. Allison¹, Simon P. Goodwin^{1*}, Richard J. Parker¹,
Simon F. Portegies Zwart², and Richard de Grijs^{3,1}

¹ *Department of Physics and Astronomy, University of Sheffield, Sheffield, S3 7RH, UK*

² *Leiden Observatory, Leiden University, PO Box 9513, 2300 RA Leiden, The Netherlands*

³ *Kavli Institute for Astronomical Astrophysics, Peking University, Beijing 100871, China*

ABSTRACT

Observations and theory both suggest that star clusters form sub-virial (cool) with highly sub-structured distributions. We perform a large ensemble of N -body simulations of moderate-sized ($N = 1000$) cool, fractal clusters to investigate their early dynamical evolution. We find that cool, clumpy clusters dynamically mass segregate on a short timescale, that Trapezium-like massive higher-order multiples are commonly formed, and that massive stars are often ejected from clusters with velocities $> 10 \text{ km s}^{-1}$ (c.f. the average escape velocity of 2.5 km s^{-1}). The properties of clusters also change rapidly on very short timescales. Young clusters may also undergo core collapse events, in which a dense core containing massive stars is hardened due to energy losses to a halo of lower-mass stars. Such events can blow young clusters apart with no need for gas expulsion. The warmer and less substructured a cluster is initially, the less extreme its evolution.

Key words: methods: N -body simulations - stars: formation - stars: kinematics and dynamics

1 INTRODUCTION

Most stars appear to form in star clusters (Lada & Lada 2003; Lada 2009; Portegies Zwart et al. 2010) and so star formation is inextricably linked with star cluster formation. Recent advances in observations and theory have allowed us to construct a basic picture of cluster formation in which clusters form dynamically cool (sub-virial), and highly sub-structured.

Clusters form in highly turbulent molecular clouds. These clouds are highly substructured, containing dense clumps and filaments (Williams 1999; Williams et al. 2000; Carpenter & Hodapp 2008) which are presumably formed by the decay of supersonic turbulence (Mac Low & Klessen 2004; Ballesteros-Paredes et al. 2007). Stars and small stellar groups form in these dense regions and are unsurprisingly observed to have a high degree of substructure when young (Larson 1995; Elmegreen 2000; Testi et al. 2000; Cartwright & Whitworth 2004; Gutermuth et al. 2005; Allen et al. 2007; Schmeja & Klessen 2006; Schmeja et al. 2008), clustering in young stellar groups has even been observed in the SMC (Schmeja et al. 2009) and LMC (Bastian et al. 2009). The same behaviour is seen in simulations of cluster formation (Klessen & Burkert 2000, 2001; Bate et al. 2003; Bonnell et al. 2003; Bate 2009;

Offner et al. 2009), including in comparison tests between AMR and SPH techniques (Federrath et al. 2010).

Clusters are observed to lose their substructure as they evolve, becoming smooth and roughly spherical (Cartwright & Whitworth 2004; Schmeja & Klessen 2006; Schmeja et al. 2008). Goodwin & Whitworth (2004) have shown that substructure can only be erased in clusters if the clusters are initially cool (sub-virial) (see also Maschberger et al. 2010). Both observations of pre-stellar cores (Belloche et al. 2001; André 2002; Walsh et al. 2004; Peretto et al. 2006; Kirk et al. 2007) and stars (Peretto et al. 2006; Proszkow et al. 2009) show that they indeed appear to be sub-virial, a property also found in simulations of cluster formation (Klessen & Burkert 2000; Offner et al. 2009; Maschberger et al. 2010).

Following Allison et al. (2009b) we conduct N -body simulations of a large number of initially sub-virial, fractal star clusters. In Section 2 we describe our simulations. In Section 3 we describe our main results, specifically the early onset of dynamical mass segregation and interesting ‘post-collapse’ evolution. In Section 4 we discuss the results, and we summarise and conclude in Section 5.

* E-mail: s.goodwin@sheffield.ac.uk

2 INITIAL CONDITIONS

We perform 160 N -body simulations with 1000 stars each, in which the initial conditions are cool and clumpy. We vary the level of substructure and initial virial ratio, and conduct ensembles of simulations with the same initial conditions, varying only the initial random number seed used to initialise the simulations.

To create initial substructure in our simulations we use a fractal stellar distribution. Using a fractal distribution provides a parameterisation of substructure using only a single number: the fractal dimension. (Note that we are not claiming that clusters are actually initially fractal, although they may be (Elmegreen & Elmegreen 2001; Cartwright & Whitworth 2004), just that this provides a simple descriptor of substructure that is easy to reproduce).

The fractal stellar distributions were generated following the method of Goodwin & Whitworth (2004). The method begins by defining a cube of side N_{div} (we use $N_{\text{div}} = 2$ throughout), inside of which the fractal will be built. A first-generation parent is placed at the centre of the cube, from which are spawned N_{div}^3 sub-cubes, each containing a first-generation child in its centre. The fractal is then built by determining which of the children themselves become parents, and spawn their own offspring. This is determined by the fractal dimension, D , where the probability that a child becomes a parent is $N_{\text{div}}^{(D-3)}$. For a lower fractal dimension less children will mature and so the final distribution will contain more structure. Any children which do not become parents in a given step are removed, along with all of their parents. A small amount of noise is then added to the positions of the remaining children, preventing the final cluster from having a gridded appearance, and the children become parents of the next generation. Each new parent then spawns N_{div}^3 second-generation children in N_{div}^3 sub-sub-cubes, with each second-generation child having a $N_{\text{div}}^{(D-3)}$ probability of becoming a second-generation parent. This process is then repeated until there are substantially more children than required. The children are pruned to produce a sphere from the cube and are then randomly removed (so maintaining the fractal dimension) until the required number of children are left. These children then become the stars in the cluster.

To determine the velocity structure of the cloud, children inherit their parent's velocity plus a random component that decreases with each generation in the fractal. The children of the first generation are given random velocities from a Gaussian of mean zero¹. Each new generation then inherits their parent's velocity plus an extra random component that becomes smaller with each generation. This results in a velocity structure in which nearby stars have similar velocities, but distant stars can have very different velocities. Finally, the velocity of every star is scaled to obtain the desired total virial ratio for the cluster.

The simulations contain 1000 stars, have an initial max-

¹ Here the variance is unimportant as the velocities are scaled to the desired virial ratio once the final spatial distribution is obtained, but the method can also be used to match the Larson (1981) relations if desired (see Goodwin & Whitworth 2004).

Q	D			
	1.6	2.0	2.6	3.0
0.3	a1.01–50	a2.01–10	a3.01–10	a4.01–10
0.4	b1.01–10	b2.01–10	b3.01–10	b4.01–10
0.5	c1.01–10	c2.01–10	c3.01–10	c4.01–10

Table 1. Notation for run identification where D is the initial fractal dimension, and Q is the initial virial ratio of each simulation. The numbers 01–50 and 01–10 are the identifiers for each individual run. Within each ensemble only the random number seed used to generate the initial conditions is changed.

imum radius of 1 pc, include no primordial binaries or gas and a three-part power law is used to produce an initial mass function (IMF, Kroupa 2002),

$$N(M) \propto \begin{cases} M^{-0.3} & m_0 \leq M/M_{\odot} < m_1, \\ M^{-1.3} & m_1 \leq M/M_{\odot} < m_2, \\ M^{-2.3} & m_2 \leq M/M_{\odot} < m_3, \end{cases} \quad (1)$$

with $m_0 = 0.08 M_{\odot}$, $m_1 = 0.1 M_{\odot}$, $m_2 = 0.5 M_{\odot}$ and $m_3 = 50 M_{\odot}$. No stellar evolution is included because of the short duration of the simulations (~ 4 Myr). We use the STARLAB N -body integrator KIRA to run our simulations (Portegies Zwart et al. 2001).

In this study we explore a range of fractal dimensions and virial ratios. The fractal dimensions investigated are $D = 1.6$, 2.0, 2.6 and 3.0 (since these values correspond to the number of maturing children, $N_{\text{div}}^D \equiv 2^D$, being an integer), where $D = 1.6$ produces a large amount of structure, and $D = 3.0$ produces a uniform sphere. We investigate virial ratios of $Q = 0.3$, 0.4 and 0.5, we define the virial ratio as $Q = T/|\Omega|$ (where T and $|\Omega|$ are the total kinetic and total potential energy of the stars, respectively), hence virial equilibrium is $Q = 0.5$.

It is important to note that fractal initial conditions are inherently stochastic: statistically identical fractals (i.e., the same fractal dimension), can appear very different to the eye, and can evolve in very different ways (see Section 3.3). Therefore, it is vital to perform large ensembles of simulations with different random number seeds. We have therefore simulated 50 $D = 1.6$, $Q = 0.3$ (a1) clusters (as they have the most interesting evolution), and restricted our analysis of all other combinations of D and Q to 10 clusters each. The identifiers and initial conditions of each ensemble are presented in table 1.

To quantify mass segregation we use the minimum spanning tree (MST) method (Allison et al. 2009a). This method compares the MST of the N most massive stars with the average MSTs of N randomly selected stars. The ratio of these two MST lengths gives a quantitative measure of the concentration of the massive stars and hence a value of the mass segregation in the cluster,

$$\Lambda = \frac{\langle l_{\text{norm}} \rangle}{l_{\text{massive}}} \pm \frac{\sigma_{\text{norm}}}{l_{\text{massive}}} \quad (2)$$

where Λ is the measure of mass segregation, $\langle l_{\text{norm}} \rangle$ is the average length of the random MSTs, l_{massive} is the length of the massive star MST and σ_{norm} is the error in the random MST length. The value $\sigma_{\text{norm}}/l_{\text{massive}}$ is the 1σ error in Λ .

In this paper, mass segregation is calculated for the entire stellar content (i.e. ejected stars are not removed from

the simulation) in all three dimensions. We note that an observer will see only two dimensions, and may not identify all cluster members, in particular low-mass stars and stars that have been ejected from the cluster. Allison et al. (2009a) show that there is little difference between the mass segregation measure in two and three dimensions when using mass segregated Plummer spheres. However, as with all mass segregation measures, if using the measure in two dimensions projection effects may cause differences depending on orientation. Unfortunately, this is unavoidable. Including all stars is useful theoretically, however it does not allow a direct comparison with observational data.

3 RESULTS

3.1 Rapid dynamical mass segregation

In Allison et al. (2009b, hereafter Paper I) we showed that cool ($Q = 0.3$), and clumpy ($D = 1.6$) clusters can dynamically mass segregate on a timescale close to the initial crossing time of the system (~ 1 Myr). Figure 1 shows the early evolution and onset of mass segregation in such a cluster. The top panels show the spatial distributions of the cluster at times $\sim 0.01, 0.81$ and 1.02 Myr (left to right), whilst the lower panels show the mass segregation ratio Λ for each of these snapshots – the higher the value of Λ , the greater the degree of mass segregation. As is clear from the figure, the cluster evolves from an initially non-mass segregated and clumpy distribution, into a smooth and mass segregated one.

In paper I we argued that this rapid dynamical mass segregation is due to the collapse of the cool cluster forming a very dense, but short-lived core (at ~ 0.8 Myr in the example shown in Fig. 1). These dense cores (for $D = 1.6$, $Q = 0.3$) tend to contain about half of the mass of the cluster, are roughly $0.1 - 0.2$ pc in radius, and survive for $0.1 - 0.2$ Myr (10 – 20 crossing times in the core).

Spitzer (1969) showed that the timescale for mass segregation, t_{seg} , for a star of mass M depends on how massive that star is relative to the average mass of a star in a cluster, $\langle m \rangle$,

$$t_{\text{seg}}(M) \approx \frac{\langle m \rangle}{M} t_{\text{relax}}, \quad (3)$$

where t_{relax} is the relaxation time of the cluster, which is related to its crossing time, t_{cross} , by

$$t_{\text{relax}} \approx \frac{N}{8 \ln N} t_{\text{cross}}. \quad (4)$$

Eq. 3 can be rewritten as

$$t_{\text{seg}} \approx \frac{\langle m \rangle}{M} \frac{N}{8 \ln N} t_{\text{cross}}. \quad (5)$$

For the $D = 1.6$, $Q = 0.3$ initial conditions used in paper I, typical values for these parameters are $N \sim 300 - 500$, $t_{\text{cross}} \sim 0.01 - 0.2$ Myr, $\langle m \rangle \sim 0.4 M_{\odot}$ (typical for standard IMFs). The core has a lifetime of $0.1 - 0.2$ Myr in which it can mass segregate giving a mass to which the core can segregate of $M \sim 2 - 4 M_{\odot}$. In Fig. 1 the cluster is mass segregated to the 20th most massive star, which has a mass of a few M_{\odot} , in good agreement with our simple analytical model.

The reason that a dense core can form is that the cluster is both cool *and* clumpy: cool clusters will initially collapse,

but cool and clumpy clusters can collapse further. The potential energy, Ω , of a cluster of mass M_{clus} and radius R is

$$\Omega = -\eta \frac{GM_{\text{clus}}^2}{R}, \quad (6)$$

where η is a structure parameter whose value depends on the choice of R (e.g., is it the core radius or the half-mass radius?), and the structure of the cluster (e.g., is it clumpy, Plummer, or uniform density?) (see also, Portegies Zwart et al. 2010). For example, for a Plummer sphere, if R is the Plummer radius then $\eta \sim 0.3$.

If a cluster has an initial potential energy Ω_0 (with radius R_0 and structure parameter η_0), and an initial virial ratio Q_0 , then the initial total energy E_0 is

$$E_0 = -\eta_0 \frac{GM_{\text{clus}}^2}{R_0} (1 - Q_0).$$

Whatever the initial conditions, a (bound) cluster will attempt to reach virial equilibrium and a relaxed configuration (something like a Plummer sphere, or King profile with a concentration parameter² $\approx 2 - 3$, for an a1 type cluster). Therefore, the final energy E_f of the cluster (with potential energy Ω_f , radius R_f , structure parameter η_f , and virial ratio $Q_f = 0.5$) will be

$$E_f = -\eta_f \frac{1}{2} \frac{GM_{\text{clus}}^2}{R_f}$$

(assuming no mass is lost). Equating these equations gives the degree of collapse (or expansion if initially warm) of the cluster

$$\frac{R_0}{R_f} = \frac{\eta_0}{\eta_f} 2(1 - Q_0). \quad (7)$$

Clearly, to induce dynamical mass segregation on a short timescale, R_0/R_f must be as large as possible to cause the maximum degree of collapse. This implies that both η_0/η_f and $2(1 - Q_0)$ need to be large.

Obviously, making $2(1 - Q_0)$ large means making Q_0 as small as possible, but even with an initially static stellar distribution with $Q_0 = 0$, $2(1 - Q_0)$ can never be greater than two (this is why Bonnell & Davis 1998 did not see rapid, early mass segregation). Realistically, it is difficult to imagine Q_0 being much less than 0.2 or 0.3 as the stars *must* initially have some relative velocities.

As stated above, the cluster will not just relax into virial equilibrium, it will also attempt to reach a basic statistical equilibrium which is a smooth, centrally concentrated distribution (like a Plummer sphere or King model if tidally truncated). Therefore the final structure parameter will be $\eta_f \sim 0.3$ when the scale radius is the Plummer radius.

Numerical experiments we have carried out show that the structure parameter for a fractal of dimension $D = 1.6$ is $\eta_0 \sim 1.1 \pm 0.1$, for $D = 2.0$, $\eta_0 \sim 0.8 \pm 0.1$ (note that different realisations of $D = 1.6$ and $D = 2.0$ fractals have a large variation in their structure parameters), for $D = 2.6$, $\eta_0 \sim 0.7$, and for $D = 3.0$, $\eta_0 \sim 0.6$. For each of these η values the scale radius is the total radius of the fractal. Unfortunately, it is very difficult to exactly compare the η of

² We define the concentration parameter as $c = \log_{10}(r_{\text{virial}}/r_{\text{core}})$

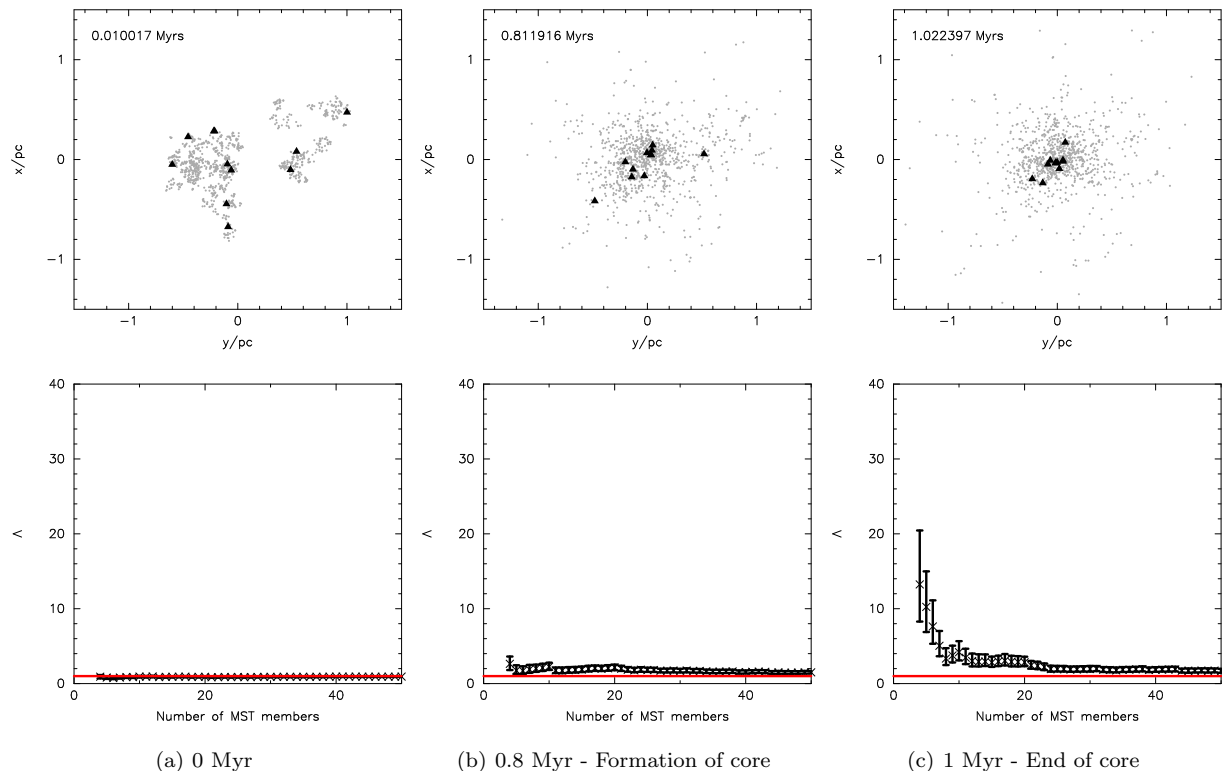


Figure 1. Run a1.34 – *Top*: 2 dimensional stellar distributions at (a) 0 Myrs - the initial distribution, (b) 0.8 Myrs - the formation of the dense core and (c) 1 Myr - the end of the dense core and initial dynamical mass segregation. Triangles indicate the positions of the 10 most massive stars. *Bottom*: The evolution of Λ with N for (a), (b), (c); as described above. The error bars show 1σ deviations.

a Plummer model and the η of a fractal as the radii are defined differently. The half-mass radius of fractal models varies quite significantly (and its meaning is also rather unclear in a fractal) and so does not provide a useful comparison radius either.

3.2 Mass segregation in clusters with different D and Q

The analysis above suggests that the initial virial ratio and the initial fractal dimension of a cluster are the crucial parameters in determining whether that cluster will be able to rapidly dynamically mass segregate. In particular, the warmer (higher- Q), and the smoother (higher- D) a cluster is, the lower the maximum central density, and hence less dynamical mass segregation will occur.

In Fig. 2 we show the typical evolution of Λ with time for clusters with different initial virial ratios and fractal dimensions for $N = 10, 20$ and 50 , the full version of this figure, showing the evolution of all of the simulations, can be found in the supplementary data. In the top left is our canonical $Q = 0.3$, $D = 1.6$ cluster from paper I. From left to right, the initial virial ratio increases from $Q = 0.3$ to 0.4 and 0.5 (virialised). From top to bottom, the fractal dimension increases from $D = 1.6$ (very clumpy) to $2.0, 2.6$ and 3.0 (roughly a uniform density sphere).

It would be expected from our earlier argument that lower- Q and lower- D clusters will collapse to a denser state, and hence show more rapid and more pronounced dynamical

mass segregation. This is exactly what is seen in Fig. 2: faster and more intense mass segregation at the top left (cool and clumpy clusters), and no appreciable mass segregation at all at the bottom right (virialised, uniform density clusters). The trend in the typical evolution of clusters in our parameter space shown in Fig. 2 is exactly what we would expect to see following the theoretical argument in Section 3.1.

Whilst the behaviour of ‘typical’ clusters is exactly what is expected, many individual clusters show unusual and unexpected behaviour. Examination of each simulation (see the supplementary data) shows that, whilst the general pattern of evolution with D and Q holds, there is a large degree of stochasticity due to each fractal being different in detail to every other fractal.

3.3 Stochasticity

The supplementary data shows that a number of simulations do not show the behaviour that we might expect for their D and Q values. The evolution of fractal clusters depends significantly on the specific initial conditions of the cluster. The systems are inherently chaotic and so each new random number seed can deliver completely different evolution. Phenomena which occur during the evolution of a cluster (such as mass segregation) can also be very transient. In some systems, Λ may change by a large factor on short timescales. In this section we have chosen a few examples which demonstrate the stochasticity and transience in the evolution of cool, clumpy clusters.

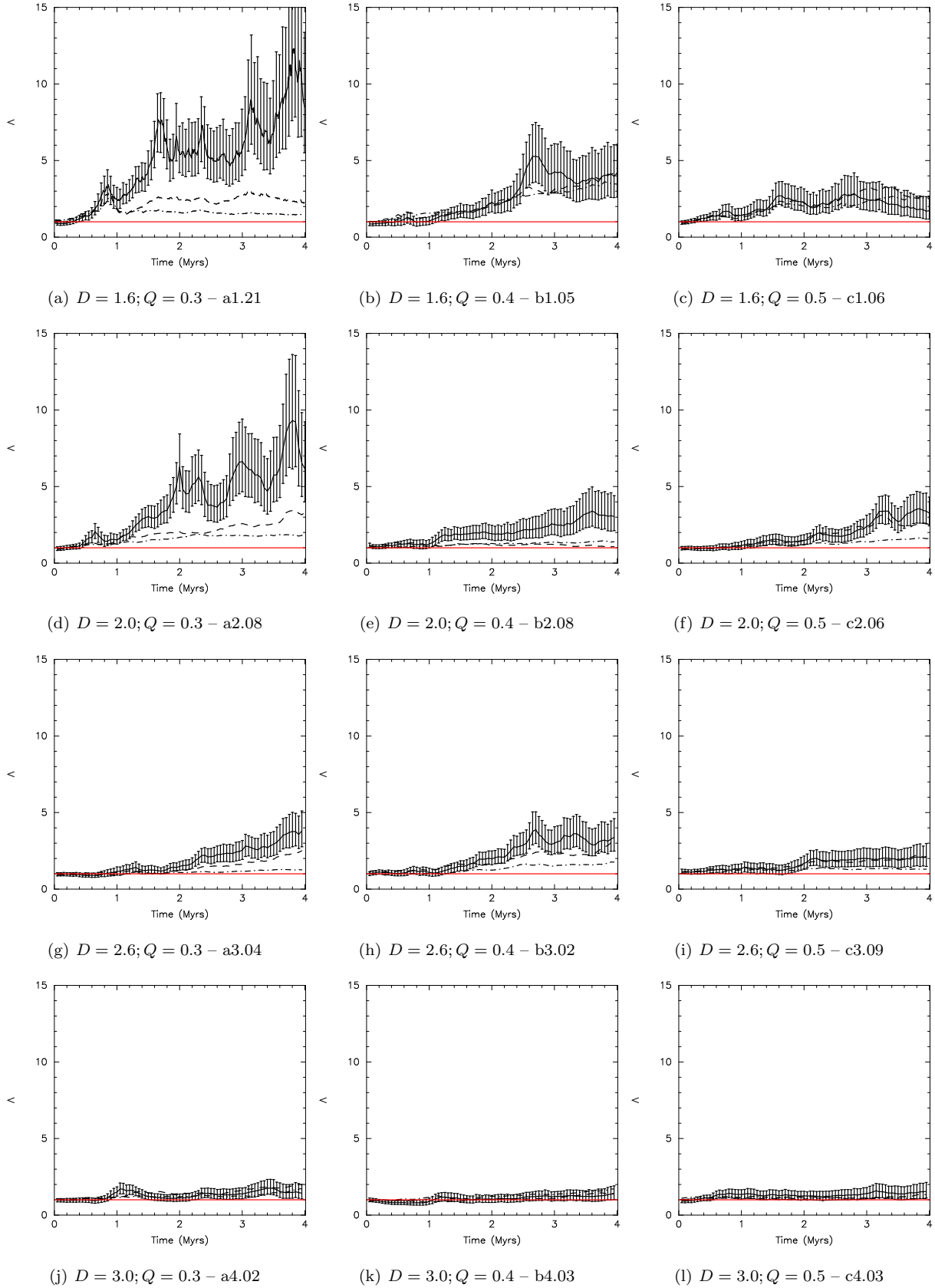


Figure 2. Generic examples from the investigated D and Q values. Plots show the evolution of mass segregation (Λ) with time for $N = 10$ (*solid*, includes error bars); $N = 20$ (*dashed*); $N = 50$ (*dot-dash*). The red line indicates a Λ of unity i.e. no mass segregation. The error bars show a 1σ deviation. A movie showing the evolution of (a) a1.21 can be downloaded at <http://www.astro.group.shef.ac.uk/stars.html>

There are several $D = 1.6, Q = 0.3$ clusters which appear to have little or no mass segregation, for example run a1.20 (see Fig. 3). In this cluster there appears to be no significant mass segregation at any time during the 4 Myr of the simulation for $N = 10, 20$ and 50. Fig. 3(b) shows the evolution of Λ for run a1.20 in more detail than Fig. 3(a). In this plot we show Λ for $N = 4, 6, 8, 10$ and 12. It is now clear that the cluster *does* mass segregate, but only for stars more massive than the 6th most massive star. In fact, a substantial multiple system consisting of the 4 most massive stars is formed in this cluster. Mass segregation is only present for the 6th most massive stars because the 7th most massive star is ejected early in the simulation, thereby enlarging the length of all MSTs that include more than 7 stars. Mass segregation for $N = 4$ occurs at 0.8 Myr with $\Lambda = 3.4^{+1.8}_{-1.5}$, and by 2 Myr Λ for the four most massive stars has risen to $50.9^{+22.0}_{-19.9}$, with a total MST length of 13000 AU (an average separation of 3250 AU), Λ is very high here because many lower mass stars have been widely spread from the cluster, making the random MSTs large. This also explains the large error values. Fig. 3(b) illustrates the rapid variations in Λ for the small- N system of the most massive stars, and the fairly smooth variation for larger N .

Superficially, run c4.10 looks very similar to run a1.20, for $N = 10, 20$ and 50, in that it shows no evidence for mass segregation throughout the simulation. When we investigate this cluster in detail, we find that the two simulations are completely different as this cluster does not undergo a dense collapse phase. It becomes only slightly mass segregated at 3.2 Myr with Λ for $N = 4$ of $3.1^{+1.5}_{-1.1}$.

In runs a1.08 and a1.21 the stochasticity of runs with different random number seeds is easily seen. Both simulations are initially *statistically* the same, but in Fig. 4 we show the states of the clusters at ≈ 1.9 Myr. Run a1.08 shows no evidence of mass segregation, whilst run a1.21 shows very significant mass segregation out to $N = 20 - 25$ (in Fig. 4(b) the 10 most massive stars are very closely clustered in the centre, and the symbols indicating their positions overlap somewhat).

It is important to note that the plots used in Fig. 2 do not show all of the mass segregation information. They only show mass segregation for the N which is plotted (in this case $N = 10, 20$ and 50). This choice is rather arbitrary and fails to provide all of the information. We have chosen to plot these values for clarity, but any detailed investigation of the evolution of cool, clumpy clusters requires an analysis of a three dimensional dataset including time, N , and Λ .

In run a1.04, the stochastic and transient nature of mass segregation can be seen. Fig. 5(a) shows that at 2.1 Myr the twelve most massive stars in the cluster are in a heavily mass segregated state. However, Fig. 5(b), shows that only 0.1 Myr later the amount of observed mass segregation in the cluster has been reduced from $\Lambda \approx 21$ to $\Lambda \approx 6$ because of the disruption of the massive multiple system at the core.

As observations are a snapshot of one time in a cluster’s evolution, they only provide two dimensions of N and Λ . This means that observations miss the time evolution of the system which, as is clear in many plots in the supplementary material, can vary extremely rapidly. Hence we stress that observations only provide a snapshot of a young cluster. *Young clusters can evolve very rapidly* on a timescale of ~ 1 Myr. Therefore the instantaneous state of a clus-

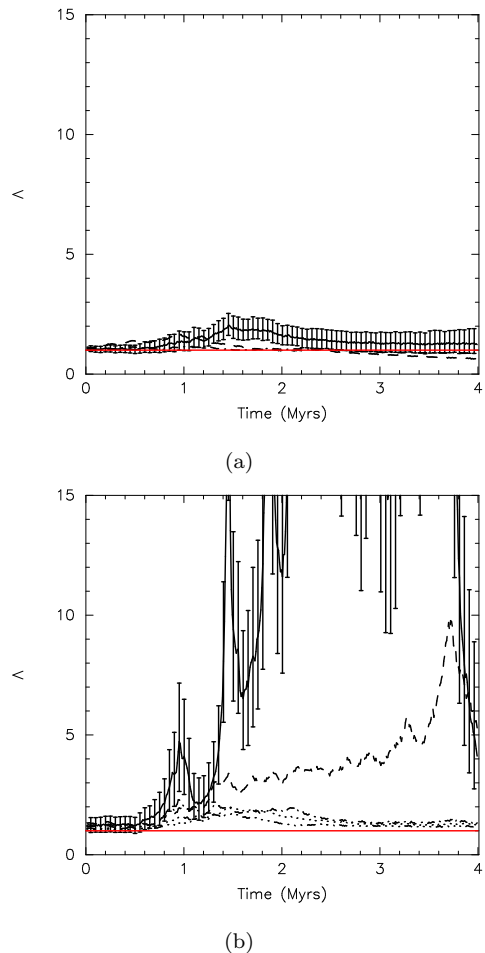


Figure 3. Evolution of Λ with time for run a1.20. Top: $N = 10, 20$ and 50. Bottom: $N = 4$ (solid line), 6, 8, 10, and 12 (top to bottom) for run a1.20. Error bars have only been included for $N = 4$ for clarity.

ter (especially if it is based on two dimensional positions) may provide no information on what the cluster was like in the recent past, or to how it might evolve in the near future (see also Goodwin & Bastian 2006; Bastian et al. 2008; Allison et al. 2009b).

3.4 Post-collapse evolution

The collapse of clumpy clusters may not lead only to mass segregation, but also to other interesting phenomena; most notably the formation of ‘Trapezium-like’ systems, the rapid ejection of massive stars, and the disruption of the cluster itself.

3.4.1 Formation of ‘Trapezium-like’ systems

The Trapezium in the Orion Nebula Cluster (ONC) is a multiple system consisting of four of the most massive stars in the ONC. For the following discussion we shall use a simple definition of a ‘Trapezium-like’ system as a close group of massive stars (at least 3 with $M > 8 M_{\odot}$) which are bound. Under this criterion, 45 of the 50 $D = 1.6, Q = 0.3$

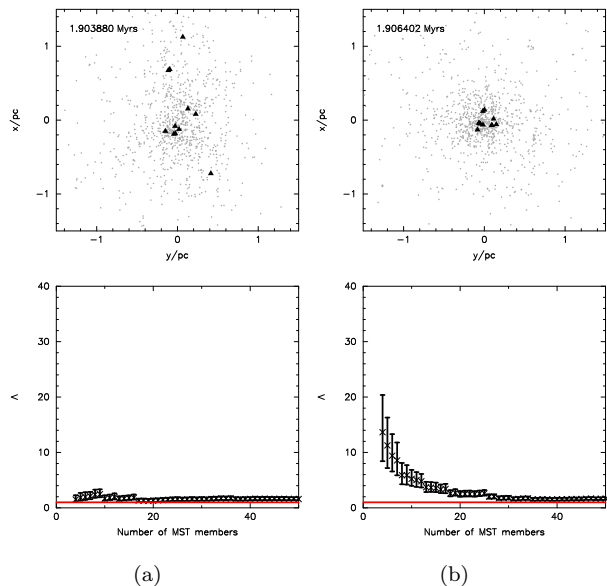


Figure 4. Runs a1.08 (a) and a1.21 (b): $D = 1.6, Q = 0.3$. The ten most massive stars are depicted by triangles. The most massive stars are not always clearly seen because of close grouping.

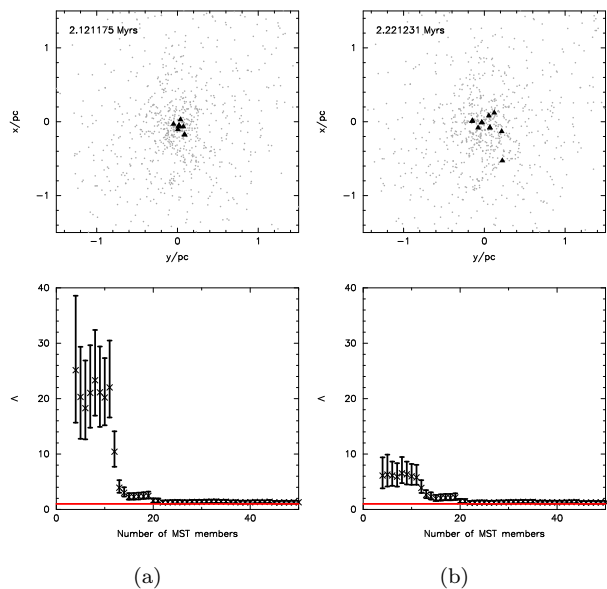


Figure 5. Run a1.04: $D = 1.6, Q = 0.3$. The ten most massive stars are depicted by triangles. (a) At 2.1 Myr the cluster shows very high levels of mass segregation for the twelve most massive stars ($\Lambda \approx 21$). The ten most massive stars are tightly grouped in the centre of the the cluster, and cannot be seen clearly. (b) 0.1 Myr later, the amount of mass segregation present in the cluster has been vastly reduced ($\Lambda \approx 6$). There are two massive star-massive star binaries in the central region, causing symbols to overlap.

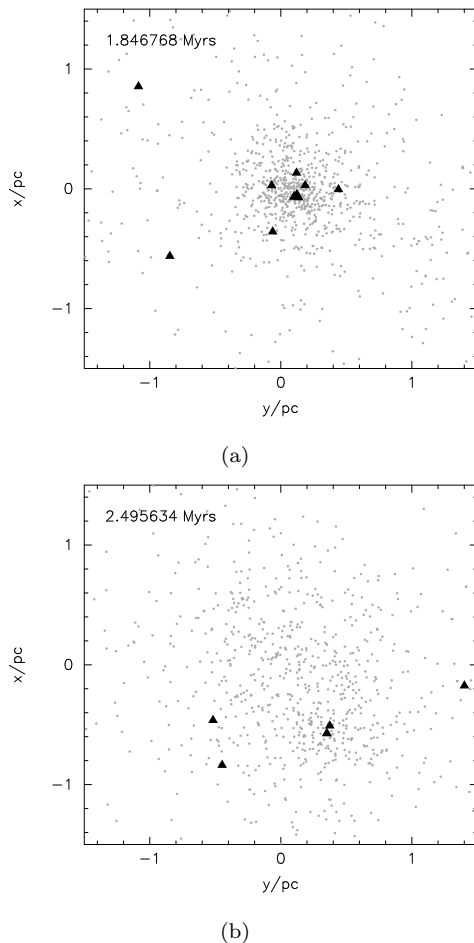


Figure 6. Run a1.02: $D = 1.6, Q = 0.3$. The ten most massive stars are depicted by triangles. (a) The cluster has evolved to form a centrally concentrated distribution. In the core there is a tight triple system consisting of 3 of the most massive stars, which cannot clearly be seen. (b) 0.7 Myr after (a), the cluster has been destroyed by the decay of the multiple system, and most of the 10 most massive stars have been ejected.

simulations formed a ‘Trapezium-like’ system. These simulations contained no primordial binaries, but were able to migrate the most massive stars into very close proximity to each other on very short timescales (~ 1 Myr) through dynamics alone (see also, Allison et al. 2009b). In the 50 $D = 1.6, Q = 0.3$ simulations, the average shortest separation reached by the four most massive stars was 0.04 pc (about 8000 AU), which occurs within the first 2 Myr. The shortest separation between the four most massive stars in any simulation was 0.0025 pc (500 AU). We would expect that with different initial conditions (i.e., initial binaries, smaller R_0 , etc) these multiple systems could be made even more extreme. In fact, preliminary investigations of simulations with an initial fractal radius of 0.5 pc (half the size used in this paper) and only single stars found a ‘Trapezium-like’ system with the four most massive stars in a cluster with an average separation of only 20 AU between them.

‘Trapezium-like’ systems form during the dense core phase as the most massive stars loose kinetic energy through two-body encounters with lower-mass stars. As they mass

segregate, the typical separations between the most massive stars decrease and they form high-order multiple systems. We note that the dense core that forms at the peak of the collapse is similar to the initial conditions used by Pflamm-Altenburg & Kroupa (2006) to model the formation of the Trapezium in the ONC. It also has the extreme density required to explain observations of η Cham (Moraux et al. 2007) and the ONC (Parker et al. 2009). We will examine the formation and evolution of ‘Trapezium-like’ systems in more detail in a subsequent paper (R. J. Allison et al., in prep.). Hydrodynamical simulations also show the formation of trapezium-like systems in the gas-dominated phase of cluster formation (see, Bonnell et al. 2003; Klessen et al. 2009). These systems are able to form due to the ability of gas to dissipate kinetic energy and redistribute angular momentum. Therefore, if the effects of gas were included in these simulations we would expect the trapezium systems which form in these simulations to appear earlier and to be even more extreme.

3.4.2 Core collapse?

Some simulations appear to show core collapse events. Early mass segregation can create a core-halo structure in the cluster, with a dense core of massive stars, surrounded by a halo of lower-mass stars. The dense core often forms a Trapezium-like system (see above). The lower-mass stars are typically on radial orbits, and may enter and extract energy from the core causing it to shrink and the higher-order massive multiples to harden. This also causes the halo to heat up and the cluster to start dissolving. At some point, the massive multiples may decay, ejecting high-mass stars at high velocity (see below) and blowing the cluster apart.

In run a1.02, for example, the cluster collapses and forms a dense core. The 4 most massive stars form a Trapezium-like system which very rapidly decays and destroys the cluster. Fig. 6(a) shows the cluster during the ‘core phase’, the massive star multiple system is in the centre of the cluster (but the individual stars are too close to resolve in this image). Fig. 6(b) shows the cluster 0.7 Myr later. Most of the massive stars have been ejected from the central 1 pc, and the cluster has been destroyed. Prior to dissolution, the degree of mass segregation increases as the central multiple hardens, and at around 1.9 Myr the central multiple finally decays, ejecting the most massive stars and creating a hard binary. This system contains two stars of mass 45.3 and 27.8 M_{\odot} , which had an initial separation of 800 AU before the ejection, and a separation of ~ 100 AU after. This binary increases its binding energy by around 1×10^{40} J, which is comparable to the entire potential energy of the cluster of $\sim -6 \times 10^{39}$ J. In this simulation the formation of the binary system alone is able to directly disrupt the cluster. It is also possible that the energy input comes from gradual interactions with massive star multiples which slowly disrupt the cluster and form a hard massive star binary.

Table 2 shows the number of simulations for which the final (4 Myr) virial ratio is greater than unity (i.e., the cluster is unbound). Energy is conserved in the simulations, but

Q	D			
	1.6	2.0	2.6	3.0
0.3	32/50	2/10	0	0
0.4	6/10	2/10	0	0
0.5	7/10	0	0	0

Table 2. Fraction of clusters which become globally unbound with varying initial virial ratio, Q , and fractal dimension, D .

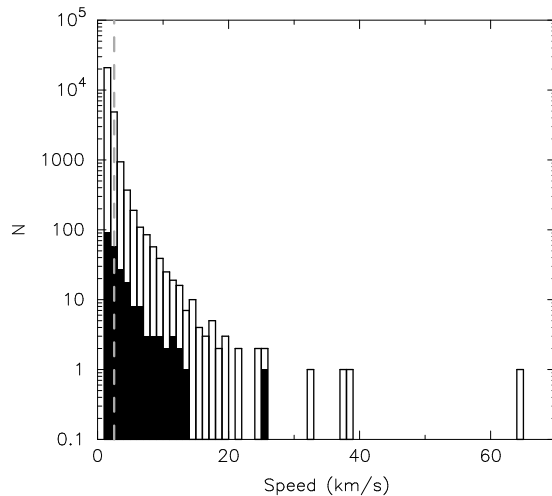


Figure 7. Distribution of final speeds of all stars from the 50 $D = 1.6, Q = 0.3$ simulations. The black region shows stars with $M > 10 M_{\odot}$, and the dashed line shows the average escape speed ($v_{\text{esc}} \approx 2.5 \text{ km s}^{-1}$).

an unbound cluster may be formed from an initially subvirial cluster through the redistribution of energy in the core collapse phase.

Even if the cluster manages to survive for the 4 Myr of our simulations, shortly after this the most massive stars will become supernovae and the loss of the most bound portions of the cluster should destroy the cluster. Thus clusters can be destroyed dynamically without the need for gas expulsion (Goodwin & Bastian 2006; Goodwin 2009).

3.4.3 Massive star ejections

The ejection of massive stars from clusters can occur in three ways. Firstly, Trapezium-like systems are inherently unstable and can decay dynamically (Sterzik & Durisen 1998). Secondly, other massive stars can interact with Trapezium-like systems or with massive binaries and be ejected. Thirdly, the hardening of Trapezium-like systems in core collapse processes may decrease its stability and cause it to decay faster than it might otherwise have done.

Figure 7 shows the final (at 4 Myr) velocity distribution of the 50 $D = 1.6, Q = 0.3$ simulations, for comparison the typical velocity dispersion of a cluster is $\sim 1.9 \text{ km s}^{-1}$, and the typical escape velocity is $\sim 2.5 \text{ km s}^{-1}$. The plot shows that it is quite possible for the massive star ejections to reach velocities in excess of 10 km s^{-1} . The simulations produce stars with masses $> 30 M_{\odot}$ having ejection velocities $> 10 \text{ km s}^{-1}$, and in one case a $12 M_{\odot}$ star is ejected with a veloc-

ity of 25.9 km s^{-1} . In all, 13 per cent of stars $> 10 M_{\odot}$ were ejected with velocities $> 5 \text{ km s}^{-1}$ ($\approx 5 \text{ pc Myr}^{-1}$).

4 DISCUSSION

Many young clusters are observed to be ‘mass segregated’, that is their most massive stars are concentrated preferentially towards their centres. The ONC (2-3 Myr) is well known to be mass segregated. Hillenbrand & Hartmann (1998) find, using the cumulative distribution of different mass groups, evidence of mass segregation for stars more massive than $5 M_{\odot}$, and a possibility that mass segregation is present for stars $> 1\text{-}2 M_{\odot}$. Allison et al. (2009a) show, using the minimum spanning tree method, that mass segregation in the ONC is split into three ‘levels’. The first contains the four most massive stars, the second stars $> 5 M_{\odot}$, and the third is a decrease towards no mass segregation below $5 M_{\odot}$. Using the radial variation of the IMF, Harayama et al. (2008) and Sharma et al. (2008) show that NGC 3603 (2.5 Myr) and NGC 1893 (4 Myr) are mass segregated, but that there is no evidence for mass segregation for stars $< 1\text{-}2 M_{\odot}$ in either cluster. Raboud & Mermilliod (1998) show, using the cumulative distribution method, that NGC 6231 (4 Myr) is mass segregated. This cluster, like the ONC, has different ‘levels’ of mass segregation. The most massive stars ($> 16 M_{\odot}$) are clearly more mass segregated than stars of lower mass, and stars with masses between 2.5 and $16 M_{\odot}$ are spatially well mixed, but more mass segregated than stars $< 2.5 M_{\odot}$. Also using the cumulative distribution method Jose et al. (2008) find evidence for mass segregation in Stock 8 (1-5 Myr), and show that it is only apparent for stars $> 1 M_{\odot}$. Using our method, Sana et al. (2010) find that the cluster Trumpler 14 (~ 4 Myr) also shows mass segregation. There is significant mass segregation for stars more massive than $\approx 10 M_{\odot}$, but no evidence for stars less massive than this.

Such observations are a strong indication that these clusters have undergone an early dense phase. The mass segregation in these clusters follows a similar profile – mass segregation is present for the most massive stars, and below some particular mass ceases to be observed – this is what we observe in our simulations.

There are two important elements that are missing from our simulations: binaries and gas. Binaries have been neglected as we wish to explore the basic gravitational physics which binaries would confuse. In future papers, we will introduce primordial binaries into our simulations. Gas has been ignored, as it is computationally extremely expensive to include and because introducing gas introduces a whole new set of parameters (the equation of state of the gas, the Mach number and power spectrum of the turbulence, etc.). But clearly gas is a vital ingredient in very young star clusters. It is what the stars form from, and it can be a significant contributor to the background potential.

From our simulations, it is not clear if massive stars might form directly in massive cores (e.g., Krumholz et al. 2007), through fragment-induced starvation (Peters et al. 2010) or due to competitive accretion (e.g., Smith et al. 2009). However, hydrodynamical simulations indicate that gravoturbulent fragmentation leads to sub-clustered and mass segregated clusters (Mac Low & Klessen

2004; Maschberger et al. 2010). Clearly, the ability of young clusters to dynamically mass segregate on a very short timescale means that massive stars do not *have* to form (or rather, build up their mass) in the core of a young cluster. Massive stars can form in subclusters or in the outskirts of clusters and within a Myr or so be very mass segregated. However, not only stars, but also gas, will be involved in the collapse of the cluster to a dense phase and so cool collapse might enhance competitive accretion. Indeed, it is difficult to imagine that some competitive accretion will not occur during the channelling of stars and gas into a very dense state. Do massive stars form in massive cores that are then dynamically mass segregated? Does competitive accretion dominate, especially during the dense collapse to form the massive stars? Do fairly massive stars form in the outskirts of clusters which are dynamically mass segregated and then have their masses increased by competitive accretion in a hybrid scenario (such a process may be occurring in simulations; see Maschberger et al. 2010)?

5 CONCLUSIONS

Observations and theory both strongly suggest that the initial conditions of star clusters are cool and clumpy. Therefore, we have conducted a large number of N -body simulations of the early (< 4 Myr) evolution of clusters with virial ratios of $Q = 0.3, 0.4$ and 0.5 (where 0.5 is virialised), and fractal dimensions of $D = 1.6, 2.0, 2.6$ and 3.0 (where 3.0 is roughly a uniform density sphere) with radii of 1 pc and 1000 members (ie. total masses of $\sim 500 M_{\odot}$). In our simulations, all members were initially single stars selected from a Kroupa IMF, and the simulations lasted for 4 Myr (so not requiring stellar evolution to be included).

We study the evolution of the star clusters with a particular emphasis on the level of mass segregation. We measure mass segregation using a minimum spanning tree to provide a quantitative measure of mass segregation and which is not biased by clumpy underlying mass distributions (Allison et al. 2009a).

This study follows that of Allison et al. (2009b), in which we showed that clusters with $Q = 0.3$ and $D = 1.6$ (i.e., very cool and extremely clumpy) undergo collapse to a short-lived but extremely dense core. This core can dynamically mass segregate the most massive stars down to a few M_{\odot} via two-body encounters before re-expanding. The re-expansion is partially driven by the increase in the velocity dispersion of the low-mass stars caused by two-body encounters.

Our main results may be summarised as follows:

- The depth of the collapse, and so the degree of mass segregation depend on both the initial virial ratio, Q , and the degree of substructure, D . Low- Q and low- D clusters can collapse to a denser state and so mass segregate more than high- Q , high- D clusters.
- Whilst there is a general trend of increasing mass segregation with lower- Q and lower- D the inherently stochastic nature of fractals means that *statistically* identical clusters may undergo very different evolution.
- Many features are extremely short-lived, and young clusters can change rapidly and violently. Observations only provide a snapshot of the evolution of a cluster and it is

dangerous to draw conclusions about the past and future state of a cluster from a single snapshot (see also Bastian et al. 2008).

- Young clusters can undergo core collapse. Early dynamical mass segregation establishes a core of massive stars (see also Pflamm-Altenburg & Kroupa 2006) and a halo of lower-mass stars. Energy loss from the core to the halo can drive the formation of massive, hard binaries and Trapezium-like multiple systems. The heating of the halo and the hardening and subsequent decay of the central multiple systems can dynamically destroy a cluster within a few Myr.

- The interactions of massive stars in the core of a young cluster can cause the ejection of even very massive stars at velocities in excess of 20 km s^{-1} . This may help explain ejections from the ONC (see also Pflamm-Altenburg & Kroupa 2006).

- The early evolution of cool, clumpy clusters is rapid, violent, and extreme. The densities of clusters (and hence their crossing and relaxation times) can change by orders of magnitude during the first few Myr of their existence. Thus the currently observed properties of young clusters are just a snapshot in the life of these clusters and extreme care must be taken in inferring the past history or future evolution of clusters from a single snapshot (see also Goodwin & Bastian 2006; Bastian et al. 2008; Allison et al. 2009b).

That young clusters are mass segregated down to a few M_{\odot} , but not below, is due to the short-lived dynamical mass segregation phase which is able to mass segregate only the most massive stars. That the ONC has an unstable high-order multiple containing four of the most massive stars can be explained by its dynamical formation during the dense phase. The ejection of high-mass stars from clusters can occur during the dense phase, or afterwards from the decay of higher-order massive multiple systems.

ACKNOWLEDGEMENTS

RJA and RJP acknowledge financial support from STFC. SPZ is grateful for the support of the Netherlands Advanced School in Astrophysics (NOVA), the LKBF and the Netherlands Organisation for Scientific Research (NWO) (via grants #643.200.503 and #639.073.803). RdG acknowledges financial support from the National Science Foundation of China under grant 11043006. We acknowledge the support and hospitality of the International Space Science Institute in Bern, Switzerland where part of this work was done as part of a International Team Programme. We would also like to thank the referee, Ralf Klessen, for his interesting and useful comments.

REFERENCES

Allen L., Megeath S. T., Gutermuth R., Myers P. C., Wolk S., Adams F. C., Muzerolle J., Young E., Pipher J. L., 2007, in Reipurth B., Jewitt D., Keil K., eds, *Protostars and Planets V The Structure and Evolution of Young Stellar Clusters*. pp. 361–376

Allison R. J., Goodwin S. P., Parker R. J., Portegies Zwart S. F., de Grijs R., Kouwenhoven M. B. N., 2009a, *MNRAS*, 395, 1449

Allison R. J., Goodwin S. P., Parker R. J., de Grijs R., Portegies Zwart S. F., Kouwenhoven M. B. N., 2009b, *ApJ*, 700, L99

André P., 2002, *ApSS*, 281, 51

Ballesteros-Paredes J., Klessen R. S., Mac Low M., Vazquez-Semadeni E., 2007, *Protostars and Planets V*, pp 63–80

Bastian N., Gieles M., Goodwin S. P., Tranco G., Smith L. J., Konstantopoulos I., Efremov Y., 2008, *MNRAS*, 389, 223

Bastian N., Gieles M., Ercolano B., Gutermuth R., 2009, *MNRAS*, 392, 868

Bate M. R., 2009, *MNRAS*, 397, 232

Bate M. R., Bonnell I. A., Bromm V., 2003, *MNRAS*, 339, 577

Belloche A., André P., Motte F., 2001, in Montmerle T., André P., eds, *From Darkness to Light: Origin and Evolution of Young Stellar Clusters Vol. 243 of Astronomical Society of the Pacific Conference Series, Kinematics of Millimeter Prestellar Condensations in the ρ Ophiuchi Protocluster*. pp 313

Bonnell I. A., Bate M. R., Vine S. G., 2003, *MNRAS*, 343, 413

Bonnell I. A., Davies M. B., 1998, *MNRAS*, 295, 691

Carpenter J., Hodapp K., 2008, *arXiv:0809.1396*

Cartwright A., Whitworth A. P., 2004, *MNRAS*, 348, 589

Elmegreen B. G., 2000, *ApJ*, 530, 277

Elmegreen B. G., Elmegreen D. M., 2001, *AJ*, 121, 1507

Federrath, C. and Banerjee, R. and Clark, P. C. and Klessen, R. S., *ApJ*, 713, 269

Goodwin S. P., 2009, *ApSS*, pp 129

Goodwin S. P., Bastian N., 2006, *MNRAS*, 373, 752

Goodwin S. P., Whitworth A. P., 2004, *A&A*, 413, 929

Gutermuth R. A., Megeath S. T., Pipher J. L., Williams J. P., Allen L. E., Myers P. C., Raines S. N., 2005, *ApJ*, 632, 397

Harayama Y., Eisenhauer F., Martins F., 2008, *ApJ*, 675, 1319

Hillenbrand L. A., Hartmann L. W., 1998, *ApJ*, 492, 540

Jose J., Pandey A. K., Ojha D. K., Ogura K., Chen W. P., Bhatt B. C., Ghosh S. K., Mito H., Maheswar G., Sharma S., 2008, *MNRAS*, 384, 1675

Kirk H., Johnstone D., Tafalla M., 2007, *ApJ*, 668, 1042

Klessen R. S., Burkert A., 2000, *ApJS*, 128, 287

Klessen R. S., Burkert A., 2001, *ApJ*, 549, 386

Klessen R. S., Krumholz, M. R., Heitsch, F., 2009, *arXiv:0906.4452*

Kroupa P., 2002, *Science*, 295, 82

Krumholz M. R., Klein R. I., McKee C. F., 2007, *ApJ*, 656, 959

Lada C. J., 2009, *arXiv:0911.0779*

Lada C. J., Lada E. A., 2003, *ARA&A*, 41, 57

Larson R. B., 1981, *MNRAS*, 194, 809

Larson R. B., 1995, *MNRAS*, 272, 213

Mac Low M., Klessen R. S., 2004, *Reviews of Modern Physics*, 76, 125

Maschberger T., Clarke, C. J., Bonnell, I. A., Kroupa P., 2010, *arXiv:1002.4401*

Moralex E., Lawson W. A., Clarke C., 2007, *A&A*, 473, 163

- Offner S. S. R., Hansen C. E., Krumholz M. R., 2009, *ApJ*, 704, L124
- Parker R. J., Goodwin S. P., Kroupa P., Kouwenhoven M. B. N., 2009, *MNRAS*, 397, 1577
- Peretto N., André P., Belloche A., 2006, *A&A*, 445, 979
- Peters, T., Banerjee, R., Klessen, R. S., Mac Low, M.-M., Galván-Madrid, R., Keto, E. R., 2010, *ApJ*, 711, 1017
- Pflamm-Altenburg J., Kroupa P., 2006, *MNRAS*, 373, 295
- Portegies Zwart S. F., McMillan S. L. W., Hut P., Makino J., 2001, *MNRAS*, 321, 199
- Portegies Zwart, S., McMillan, S., Gieles, M., 2010, *arXiv:1002.1961*
- Proszkow E., Adams F. C., Hartmann L. W., Tobin J. J., 2009, *ApJ*, 697, 1020
- Raboud D., Mermilliod J.-C., 1998, *A&A*, 333, 897
- Sana, H., Momany, Y., Gieles, M., Carraro, G., Beletsky, Y., Ivanov, V. D., De Silva, G., James, G., 2010, *arXiv:1003.2208*
- Schmeja S., Klessen R. S., 2006, *A&A*, 449, 151
- Schmeja S., Kumar M. S. N., Ferreira B., 2008, *MNRAS*, 389, 1209
- Schmeja S., Gouliermis D. A., Klessen R. S., 2009, *ApJ*, 694, 367
- Sharma S., Pandey A. K., Ogura K., Aoki T., Pandey K., Sandhu T. S., Sagar R., 2008, *AJ*, 135, 1934
- Smith R. J., Longmore S., Bonnell I., 2009, *MNRAS*, pp 1502
- Spitzer L. J., 1969, *ApJ*, 158, L139
- Sterzik M. F., Durisen R. H., 1998, *A&A*, 339, 95
- Testi L., Sargent A. I., Olmi L., Onello J. S., 2000, *ApJ*, 540, L53
- Walsh A. J., Myers P. C., Burton M. G., 2004, *ApJ*, 614, 194
- Williams J., 1999, in Franco J., Carraminana A., eds, *Interstellar Turbulence The Structure of Molecular Clouds: are they Fractal?*. pp 190
- Williams J. P., Blitz L., McKee C. F., 2000, *Protostars and Planets IV*, pp 97